Nitrate-inducible MdBT2 acts as a restriction factor to limit apple necrotic mosaic virus genome replication in Malus domestica

Zhenlu Zhang[1], Yin-Huan Xie[1], Ping Sun[1], Fu-Jun Zhang[1], Peng-Fei Zheng[1], Chun-Xiang You[1], and Yu-Jin Hao[1]

[1]Shandong Agricultural University

April 05, 2024

Abstract

Apple necrotic mosiac virus (ApNMV) is a newly identified causal agent that is highly associated with the occurrence of apple mosaic disease in China. However, resistance gene against this virus has not been identified yet. We reported here that nitrate treatment destablized viral protein 1a via the ubiquitin-proteasome pathways to restrain ApNMV genomic RNA accumulation. A nitrate-responsive BTB/TAZ domain-containing protein MdBT2 was identified in a yeast-two-hybrid screening of apple cDNA library using viral protein 1a as bait, and 1a was confirmed to interact with MdBT2 both in vivo and in vitro. MdBT2 was further verified to promote the ubiquitination and degradation of viral protein 1a through the proteasome pathways in a MdCUL3A-scaffold protein in E3 ligase complex-independent manner. Viral genomic RNA accumulation was decreased in MdBT2 overexpression transgenic apple leaves but enhanced in MdBT2 antisense leaves compared to that in wild type. Moreover, MdBT2 was found to interfere with the interactions between viral replication proteins 1a and 2apol by competing with the latter. Taken together, our work demonstrated that nitrate-inducible MdBT2 functioned as a limiting factor in ApNMV viral RNA accumulation by promoting the ubiquitination and degradation of viral protein 1a and interfering with the interactions between viral replication proteins.

Nitrate-inducible MdBT2 acts as a restriction factor to limit apple necrotic mosaic virus genome replication in *Malus domestica*

Zhenlu Zhang*, Yin-Huan Xie, Ping Sun, Fu-Jun Zhang, Peng-Fei Zheng,

Chun-Xiang You, Yu-Jin Hao*§

State Key Laboratory of Crop Biology, College of Horticulture Science and Engineering, Shandong Agricultural University, Tai'an 271000, P.R. China

Zhenlu Zhang, zhangzhenluwenchao@163.com;

Yin-Huan Xie, 2401668263@qq.com;

Ping Sun, sunping_89@126.com;

Fu-Jun Zhang, 842326928@qq.com;

Peng-Fei Zheng, 1159332359@qq.com;

Chun-Xiang You, youchunxiang@sdau.edu.cn;

Yu-Jin Hao, haoyujin@sdau.edu.cn

***** Correspondence: Zhenlu Zhang,

zhangzhenluwenchao@163.com

Yu-Jin Hao, haoyujin@sdau.edu.cn

§ the author has been passed away.

Abstract Apple necrotic mosiac virus (ApNMV) is a newly identified causal agent that is highly associated with the occurrence of apple mosaic disease in China. However, resistance gene against this virus has not been identified yet. We reported here that nitrate treatment destablized viral protein 1a via the ubiquitin-proteasome pathways to restrain ApNMV genomic RNA accumulation. A nitrate-responsive BTB/TAZ domain-containing protein MdBT2 was identified in a yeast-two-hybrid screening of apple cDNA library using viral protein 1a as bait, and 1a was confirmed to interact with MdBT2 both in vivo and in vitro. MdBT2 was further verified to promote the ubiquitination and degradation of viral protein 1a through the proteasome pathways in a MdCUL3A-scaffold protein in E3 ligase complex-independent manner. Viral genomic RNA accumulation was decreased in *MdBT2* overexpression transgenic apple leaves but enhanced in*MdBT2* antisense leaves compared to that in wild type. Moreover, MdBT2 was found to interfere with the interactions between viral replication proteins 1a and $2a^{pol}$ by competing with the latter. Taken together, our work demonstrated that nitrate-inducible MdBT2 functioned as a limiting factor in ApNMV viral RNA accumulation by promoting the ubiquitination and degradation of viral protein 1a and interfering with the interactions between viral replication proteins.

Keywords ApNMV, *Malus domestica* , MdBT2, ubiquitination, viral genomic RNA replication, viral-host interactions

Acknowledgments

This study was financially supported by the National Natural Science Foundation of China (31901988), China Postdoctoral Science Foundation (2019M662413, 2020T130388), and Shandong Postdoctoral Innovation Project (201902042).

Abbreviations

ApNMV apple necrotic mosaic virus

MP movement protein

MET methyltransferase

RdRp RNA-dependent RNA polymerase

BMV brome mosaic virus

VRC viral replication complex

UPS ubiquitin proteasome system

CRL cullin-RING ligase

Y2H yeast two hybrid

BiFC Bimolecular fluorescence complementation

Co-IP Co-immunoprecipitation

Introduction

Apple mosaic disease is one the major and widely distributed viral diseases affecting apple growth and production all over the world. The causal agent of the disease was traditionally believed to be apple mosaic virus (ApMV), which belongs to the genus *Ilarvirus* , family*Bromoviridae* (Bujarski et al., 2012). However, recent studies revealed that apple necrotic mosaic virus (ApNMV), other than ApMV, is highly associated with the occurrence of apple mosaic disease in China (Noda et al., 2017; Xing et al., 2018), whose apple production accounts for half of the world.

ApNMV is in the same genus with ApMV, and both of them share the same genomic structure (Noda et al., 2017). They have three positive single-stranded genomic RNAs (RNA1, RNA2, and RNA3) and an encapsidated subgenomic RNA4 derived from RNA3 (Noda et al., 2017). RNA1 encodes the 1a protein, which is characterized with an N-terminal methyltransferase (MET) domain and a C-terminal NTP-binding helicase (HEL) domain. RNA2 encodes the viral RNA-dependent RNA polymerase (RdRp, $2a^{pol}$). The movement protein (MP) is encoded by the RNA3, while the coat protein (CP) is encoded the subgenomic RNA4 (Bujarski et al., 2012). Based on a well-characterized model virus brome mosaic virus (BMV), which belongs to the same family and shares similar genomic structure with ApNMV, 1a is a multifunctional protein playing essential roles in virus replication, including inducing the formation of viral replication complex (VRC), recruiting $2a^{pol}$ and template RNAs into these VRCs, and facilitating the viral genomic RNA replication (Diaz and Wang, 2014).

In natural environments, plants face continuous biotic and abiotic stresses that compromise their survival. To counteract these environmental challenges, plants have evolved various complex and efficient mechanisms of resistance, including the ubiquitin proteasome system (UPS) that is highly conserved among eukaryotes (Zhou and Zeng, 2017; Adams and Spoel, 2018). The UPS is an enzymatic process in which ubiquitin moieties are covalently conjugated to substrate proteins for degradation by proteasome, and this process has been demonstrated to play key roles in many intracellular biological processes of plants (Bachmair et al., 2001; Vierstra 2009; Alcaide-Loridan and Jupin, 2012). The ubiquitination process is mediated by a series of enzymes including an ubiquitin-activating enzyme (E1), an ubiquitin-conjugating enzyme (E2), and an ubiquitin E3 ligase (E3). Among them, E3 is a key component for targeting specificity by interacting with target substrates and transferring ubiquitins from E2 to the targets, and thus, generating the ubiquitin modification (Metzger et al., 2014). Based on the composition and activation mechanisms, four types of E3 ligases are mainly found in plants, including HECT (homologous to E3 associated protein C-terminus), RING (really interesting new gene), U-box, and CRLs (cullin-RING ligases) (Mazzucotelli et al., 2006; Vierstra, 2009). CRLs are the most abundant E3 ligases in plants and they exist as complexes with a cullin (CUL) subunit serving as molecular scaffold, and three types of CUL (CUL1, CUL3, and CUL4) have been reported in various plants (Hotton and Callis, 2008).

BTB (bric-a-brac, tramtrack and broad complex) type E3 ligase is one of the CRL subfamilies (Vierstra, 2009). In the CUL3-RING E3 ligase (CRL3) of model plant *Arabidopsis thaliana* , BTB/POZ (poxvirus and zinc finger) domain-containing proteins directly interact with both the CUL3 and substrate target, and thus serve as the substrate receptor to select proteins for degradation via the UPS (Hua and Vierstra, 2011; Genschik et al., 2013). A body of evidences has been reported to reveal the critical roles of BTB/POZ domain-containing proteins in multiple intracellular processes. For instance, BTB-BACK domain protein POB1 regulated plant immunity by interacting with and targeting PUB (Plant U-box) 17 and PUB29 for degradation in *Nicotiana benthamiana* (Orosa et al., 2017) and apple (*Malus domestica*) (Han et al., 2019), respectively. In Arabidopsis, AtBT2 contains an N-terminal BTB/POZ domain, a central TAZ (transcriptional adaptor zinc finger) domain, and a C-terminal calmodulin-binding domain (Ren et al., 2007). AtBT2 has been reported to be involved in regulation of multiple responses, such as responding to circadian, light, stresses, and nutrients; suppressing the sugar signaling; modulating plant hormone responses by suppressing abscisic acid (ABA) signaling while enhancing auxin signaling; and regulating telomerase activity by acting downstream of TAC1 (TELOMERASE ACTIVATOR1) (Ren et al., 2007; Mandadi et al., 2009; Kunz et al., 2015; Misra et al., 2018). MdBT2, a homologue of AtBT2, shares similar protein structure with AtBT2, and has also been demonstrated to function as a signal hub to regulate anthocyanin biosynthesis, leaf senescence, iron homeostasis, and malate accumulation in response to multiple hormonal and environmental signals (Zhao et al., 2016; An et al., 2019a; An et al., 2020 a; Zhang et al., 2020 a, b). For example, MdBT2 interacts with and promotes the ubiquitination and degradation of MdMYB1 and MdCIbHLH1 to inhibit accumulation of anthocyanin (Wang et al., 2018) and malate (Zhang et al., 2020 a, b), respectively, in response to nitrate. In addition, MdBT2 functions in delaying the leaf senescence by interacting with and promoting the ubiquitination and degradation of MdbHLH93 and MdMYC2 in apple (An et al., 2019 a; An et al., 2021).

Nitrogen (N) is a major nutrient for plant growth and productivity, and it has been reported to play key roles in plant immunity by regulating plant resistance against various pathogens (Dordas, 2008). To date, a well known defense-related N-derivant is nitric oxide (NO), which is partially generated through nitrate reductase (NR), a key enzyme in nitrate assimilation. Multiple evidences have demonstrated the roles of NO in transcriptional regulation of defense genes encoding pathogen-related (PR) proteins or proteins involved in phytoalexin synthesis, post-translational protein modifications, and salicylic acid (SA) accumulation (reviewed in Wendehenne et al., 2014). For example, NO was functional in brassinosteroid (BR)-mediated resistance against virus infection in *N. benthamiana* (tobacco mosaic virus, TMV) (Deng et al., 2016) and Arabidopsis (cucumber mosaic virus, CMV) (Zou et al., 2018). Additionally, nitrate, an inorganic nitrogen that is usually taken up by roots from aerobic soil, was also proved to be involved in disease resistance. For example, application of NO_3^- efflux inhibitor delayed and reduced the hypersensitive cell death triggered by cryptogein in tobacco, which was accompanied by the suppression of induction of some defense-related genes (Wendehenne et al., 2002). Moreover, feeding the tobacco plants with NO_3^- enhanced the accumulation of SA and expression of *PR1* gene, as well as the speed of cell death upon infection of *Pseudomonas syringae* pv.*Phaseolicola* (Gupta et al., 2013). All these reports revealed the potential role of nitrogen in resistance against pathogens.

In this study, we found that a nitrate-responsive protein MdBT2 interacted with ApNMV protein 1a, and promoted its ubiquitination and degradation through 26S proteasome pathways in a MdCUL3A-independent manner. ApNMV genomic RNA accumulation was inhibited in *MdBT2*overexpression (*MdBT2-OE*) transgenic apple leaves but enhanced in*MdBT2* antisense (*MdBT2-anti*) compared to that in the wild-type (WT). In addition, MdBT2 interfered with the interaction between 1a and $2a^{pol}$ through competitive interacting with 1a.

Materials and Methods

Plant materials and growth conditions

Tissue cultured seedlings of apple (*Malus domestica* cv 'Royal Gala') 'GL3' was utilized in this study (Dai et al*.,* 2013). The*MdBT2-OE* and MdBT2-anti transgenic plantlets were obtained in our previous work and kept in our lab (Wang *et al.,* 2018). The WT and transgenic 'GL3' plantlets were grown on Murashige-Skoog (MS) medium supplemented with 0.2 mg/L GA (gibberellin), 0.6 mg/L 6-BA (6-benzylamino-purine), and 0.2 mg/L NAA (naphthylacetic acid) at 25 °C under long-day (16 h : 8 h/light : dark) conditions (Wang et al.,2018). The *MdBT2-OE* (pIR-MdBT2-GFP) and *MdBT2-anti*(pIR-MdBT2) transgenic apple calli, as well as the *MdCUL3A*overexpression apple calli, were generated previously and kept in our lab (Wang et al*.,* 2018; Zhao et al, 2016). The WT and transgenic apple calli 'Orin' were cultured on MS medium containing 0.4 mg/L 6-BA and 1.5 mg/L 2,4-D (2,4-dichlorophenoxyacetic acid) at 25 °C under constant dark conditions. The *N. benthamiana* were maintained in growth chamber with 16 h : 8 h/light : dark in 23 °C.

Plasmid construction and Agrobacterium-mediated transformation

All PCR amplified fragments were first inserted into pEASY-Blunt-Simple (TransGen Biotech) cloning vector, and then constructed into expression vectors. The coding sequences of viral proteins and MdBT2 were inserted into pGAD424 and pGBT9 for yeast-two-hybrid (Y2H) assay. 1a, MdBT2, and $2a^{pol}$ were constructed into pGEX-4T-1 and pET-32a to obtain the GST- and -HIS tagged fusion proteins for pull-down assay. For the bimolecular fluorescence complementation (BiFC) assay, 1a and MdBT2 were constructed into 35S::SPYCE-cYFP and 35S::SPYNE-nYFP to obtain the 1a-cYFP and MdBT2-nYFP, respectively (Walter et al*.,* 2004). Similarly, the coding sequences of 1a, MdBT2, and $2a^{pol}$ were inserted into pGreenII 62-SK-nLuc/-cLuc for luciferase complementation imaging assay (Chen et al*.,* 2008). The coding sequence of 1a and MdBT2 were inserted into pCXSN-HA to obtain the pCXSN-1a-HA and pCXSN-MdBT2-HA (Chen et al*.,* 2009). The plant binary vectors used this work were driven by cauliflower mosaic virus (CaMV) 35S promoter. All the primers used for plasmid construction were listed in Table S1.

The three segments of ApNMV were amplified from the ApNMV-Lw we isolated previously (Zhang et al, 2020), and were constructed into modified pCAMBIA1300 binary vector, in which the viral genes were driven

by double 35S promoter.

For Agrobacterium-mediated transformation, the appropriate binary constructs were transformed into *Agrobacterium tumefaciens* strain LBA4404 and cultured in Lysogeny Broth medium supplemented with corresponding antibiotics.

Analysis of gene expression

Total RNAs of apple shoots under different treatments were extracted using an OminiPlant RNA kit (CoWin Biosciences) per manufacture's instruction. The first-strand cDNA was synthesized using the PrimeScript First Strand cDNA Synthesis Kit (TaKaRa) per manufacture's instruction.

Quantitative real-time PCR (qRT-PCR) reaction solutions (20 μl) were assembled by combining the forward and reverse primers (0.25 μM for each), template cDNA (50 ng), and SYBR Green PCR Master Mix (10 μl). The reactions (95 °C, 5 min; 95 °C, 15 s, 60 °C, 1 min, for 40 cycles) were performed using the iCycler iQ5 Detection System (Bio-Rad). 18S rRNA served as internal control. The relative gene expression was calculated using the $2^{-\Delta\Delta^{\wedge}\tau}$ methods. Three biological repeats were performed for each individual experiments. Primers used for qRT-PCR were listed in Table S2.

Yeast-two-hybrid (Y2H) assays

The Y2H studies were performed as reported by Wang et al (2018). Briefly, the cDNA library was constructed by the Oebiotech Company using the apple skin. The coding sequences of the targets, including the viral $2a^{pol}$, MP, and CP, as well as truncated MdBT2 and ApNMV 1a, were amplified and inserted into pGAD424 and pGBT9 vectors. Different combinations of bait and prey constructs were co-transformed into yeast (Y2H Gold, Clontech), and then cultured on defective medium lacking lucine (Leu) and tryptophan (Trp) at 28 °C for 2-3 d. The yeast colonies were then transferred onto selection medium without Leu, Trp, histdine (His), and adenine (Ade) to determine the interactions between bait and prey proteins.

Bimolecular fluorescence complementation (BiFC) assay

Coding sequence of ApNMV 1a and MdBT2 were inserted into 35S::SPYCE-cYFP and 35S::SPYNE-nYFP vectors (Walter et al*.,* 2004), respectively. The constructs were transformed into Agrobacterium LBA4404 and co-infiltrated into *N. benthamiana* leaves. YFP (yellow fluorescent protein) signals were observed under a confocal microscope (Zeiss, LSM880) two days post-infiltration. Different signals were obtained under the "best signal" mode, and images were acquired through single optical sections in the "Frame" mode, with a scan speed of 6 (the scan time was about 10 s).

Luciferase complementation imaging assay

Coding sequences of ApNMV 1a and MdBT2 were constructed into pGreenII 62-KS-cLuc and -nLuc vectors (Chen et al*.,* 2008), respectively. The recombinants were transformed into Agrobacterium LBA4404 and co-infiltrated into *N. benthamiana* leaves. Two days post-infiltration, the substrate of luciferase was sprayed on the leaves and incubated in dark for 3 min. Bioluminescent signals were detected under an in vivo imaging system (IVIS, Lumina II). In the IVIS acquisition control panel, 'Luminescent' was selected as 'Imaging mode', and the exposure time was set to 30 s. After photographs were acquired, a color scale, which is shown as a color bar on the right side of the images, was adjusted to improve the contrast of the images.

For the competitive assay, coding sequences of ApNMV 1a and $2a^{pol}$ were inserted into the pGreenII 62-KS-nLuc and -cLuc vectors as described previously, while MdBT2 was constructed into a pCXSN-HA vector (Chen et al*.,* 2009), and all the constructs were transformed into Agrobacterium LBA4404. The $Abs_{600}$of Agrobacterium containing 1a-nLuc and cLuc-$2a^{pol}$ was adjusted to 0.5, and combined with different ratio of pCXSN-MdBT2-HA as indicated in Fig. 6B, then co-infiltrated into *N. benthamiana*leaves. The Agrobacterium harboring pCXSN-HA plasmid served as control. The images were acquired as previously described.

Pull-down analysis

The full-length cDNAs of ApNMV 1a and MdBT2 were amplified and inserted into pGEX-4T-1 and pET-32a vectors, respectively. The constructs were then transformed into *Escherichia coli* BL21 (DE3) to induce the production of GST- and -HIS tagged fusion proteins under treatment of isopropyl β-D-1-thiogalactopyranoside at 28 °C for 6 h. The GST-1a and MdBT2-HIS fusion proteins were premixed for 1 h at 4 °C with gentle shaking. The protein mix was combined with the glutathione (GSH)-attached beads (BEAVER), and then incubated at 4 °C for 1 h with gentle shaking. After washing the beads for five times to remove the non-specific proteins, the binding proteins were eluted from the magnetic separated agarose beads with GSH solution and boiled for 5 min. The supernatant was then used for sodium dodecyl sulfate-polyacrylamide gel electrophoresis (SDS-PAGE) and immunoblotted with specific antibodies.

For competitive pull-down assay, same amount (2 μg) of GST-2a^{pol} and 1a-HIS were mixed with simple HIS-tag protein (2 μg, served as control) or different concentrations (2 μg and 6 μg) of MdBT2-HIS fusion protein, and premixed at 4 °C for 1 h with gentle shaking. Then following the protocol of pull-down assay described previously, the binding proteins were resuspended in GSH solution and used for SDS-PAGE, then detected by immunoblotting with anti-GST (Abmart) and anti-HIS (Abmart) antibodies.

Protein extraction and Western blot

The total proteins were extracted from apple tissues, including apple calli and leaves, using the protein extraction solution: 100 mM Tris-HCl (pH 7.5), 1 mM ethylenediaminetetraacetic acid disodium salt, 1% polyvinylpyrrolidone K30, 0.07% β-mercaptoethanol, and 6.85% sucrose. Prepared protein samples were separated on a 10% gel using SDS-PAGE and transferred to polyvinylidene difluoride membranes (Roche). Then specific antibodies were applied to detect corresponding proteins, and peroxidase-conjugated secondary antibodies (Adcam) were utilized to visualize the immunoreactive proteins through an ECL detection kit (Millipore). MdACTIN was used as loading control.

Co-immunoprecipitation (Co-IP) assay

Co-IP assay was performed using the BeaverBeads protein A/G immunoprecipitation Kit (BEAVER Biomedical Engineering) per manufacture's protocol. Briefly, both the beads and antibodies were pre-treated with binding buffer supplied in the kit, then the extracted total protein was mixed with the pre-treated antibodies and beads, and incubated overnight at 4 °C with gentle shaking. After five times' washing, the beads were magnetic separated and resuspended in elution buffer containing coomassie brilliant blue. The precipitates were boiled for 5 min and applied to SDS-PAGE for further analysis.

Ubiquitination assay

For detection of ubiquitinated ApNMV 1a in vivo, Agrobacterium harboring pCXSN-1a-HA construct or ApNMV infectious clone was transformed into apple leaves of WT, *MdBT2-OE* , and *MdBT2* MdBT2-anti, respectively, via vaccum technique. The leaves were kept on MS medium for five days and then collected for protein extraction after treated with 50 μM MG132 for 10 h. The total protein was immunoprecipitated using anti-HA antibody (Abmart) or anti-1a specific antibody using BeaverBeads protein A/G immunoprecipitation Kit (BEAVER Biomedical Engineering) per manufacture's protocol. The precipitates were then applied to western blot, and anti-HA, anti-1a, and anti-Ubi (Sigma-Aldrich) antibodies were utilized to detect the target proteins as described previously.

For detection the ubiquitinated ApNMV 1a in vitro, total protein were first extracted from 35S::MdBT2-GFP transgenic apple calli pretreated with 50 μM MG132 for 10 h. Then MdBT2-GFP active proteins were precipitated by anti-GFP antibody (Abmart) using BeaverBeads protein A/G immunoprecipitation Kit (BEAVER Biomedical Engineering) per manufacture's protocol. The ApNMV 1a-HIS protein obtained from prokaryotic expression system was incubated with or without MdBT2-GFP active proteins in incubation buffer at 30 °C for 12 h. The incubation buffer consists of 50 mM Tris (pH 7.5), 2 mM dithiothreitol (DTT), 50 mM $MgCl_2$, 2 mM ATP, 100 ng human E1 (recombinant human His6 UBE1, BostonBiochem), 100 ng human E2 (recombinant human UbcH5b/UBE2D2, BostonBiochem), and 1 μg ubi (recombinant human Myc Ubiquitin, BostonBiochem). The target protein ubiquitination were detected using the anti-HIS (Abmart)

and anti-Ubi (Sigma-Aldrich) antibodies.

Cell-free degradation assay

The 1a-HIS protein was obtained from prokaryotic expression system using*E. coli* BL21 (DE3). Total proteins were extracted from apple calli using degradation buffer: 25 mM Tris-HCl (pH 7.5), 10 mM NaCl, 10 mM $MgCl_2$, 5 mM DTT, 10 mM ATP, and 4 mM phenylmethysulfonyl fluoride (Wang et al*.,* 2009). The concentration of collected protein supernatants and 1a-HIS were measured using the Bradford reagent (Bio-Rad). Then 100 ng 1a-HIS protein and 300 ng total proteins were mixed and incubated at 22 °C for the indicated time. For the proteasome inhibition assay, the mixed proteins were pretreated with proteasome inhibitor MG132 (50 μM) for 30 min, while dimethyl sulfoxide (DMSO) served as mock. Then protein mixture was collected at indicated time points and the reactions were stopped by SDS-PAGE loading buffer and boiled for 5 min. The samples were then applied to western blot assay for protein degradation analysis. The results were quantified using Quantity One 1-D Analysis software (Bio-Rad).

RNA extraction and Northern Blot

The total RNAs for northern blot were extracted using hot phenol method (Kohrer and Domdey, 1991). Then equal amount (15 μg) of RNAs were used for electrophoresis and transferred to nylon membranes. Digoxigenin (DIG)-labeled probes targeting the CP-coding sequence of ApNMV were generated and used for hybridization to detect the positive-strand RNA3 ((+)RNA3) and (+)RNA4 per manufacture's protocol (Roche). Anti-DIG antibody (conjugated with alkaline phosphatase, Roche) was used for immunoblotting and a chemiluminescent substrate for alkaline phosphatase was applied for imaging through a gel imager (Bio-RAD).

Results

Nitrate treatment decreases ApNMV viral RNA accumulation

In addition to be a critical nutrient for plant growth and development, nitrate also functions as an important signal molecule to regulate expression of multiple genes in response to various environmental factors (Scheible et al*.,* 2004; Ho et al*.,* 2009) and in regulating plant resistance against pathogens (Dordas, 2008; Gupta et al., 2013; Wendehenne et al., 2002). To determine if nitrate has any effect in ApNMV infection, we first constructed the infectious clone of ApNMV by inserting the full length of ApNMV RNA1, RNA2, and RNA3 into a binary vector that driven by a double CaMV 35S promoter, respectively (Fig. 1A). The recombinant constructs were then introduced into Agrobacterium separately and co-transformed into apple plantlets leaves under different nitrate concentrations via vacuum method. Then the viral RNA accumulation were tested by Northern blot using DIG-labeled probes targeting the CP-coding sequence, and found that the RNA levels decreased with the increased concentration of KNO_3 (Fig. 1B). When the concentration of KNO_3 increased to 10 mM, the (+)RNA3 accumulation decreased to around 20% compared to that of 0 mM (Fig. 1B), suggesting high level of nitrate inhibited ApNMV viral genomic RNA replication.

Nitrate treatment destablizes viral 1a protein through the UPS pathways

Because replication proteins play key roles in viral genomic RNA duplication, we next tested the effects of nitrate on the proteins levels of 1a and $2a^{pol}$, the two assumed replication proteins of ApNMV, both in vivo and in vitro. By using the anti-1a specific antibody, we found the protein levels of 1a decreased with the increased concentration of KNO_3 (Fig. 2A), which is consistent with the RNA accumulation (Fig. 1B). Then a cell-free degradation system was utilized to test the effect of nitrate on the protein stability of both 1a and $2a^{pol}$. Increased transcript levels of *MdNRT1.1* (Ho et al*.,* 2009) and*MdBT2* (Wang et al., 2018; An et al., 2020), two representative genes that were reported in response to nitrate, under KNO_3 confirmed that these apple plantlets were indeed responded to nitrate treatment (Supplementary Fig. S1). Then same amount of 1a-HIS or $2a^{pol}$-HIS fusion proteins obtained from the prokaryotic expression system were mixed with total proteins extracted from 'GL3' leaves treated with KNO_3 or KCl, and incubated for different time. Western blot analysis showed that 1a-HIS protein degradation speed was faster in proteins extracted from KNO_3-treated 'GL3' leaves than that from KCl treatment (Fig. 2B), while the protein degradation of

$2a^{pol}$-HIS were similar between proteins extracted from KCl- and KNO3-treated leaves (Supplementary Fig. S2A), suggesting nitrate treatment compromised the protein stability of 1a but not $2a^{pol}$.

The UPS-mediated protein degradation is one of the most common and powerful pathways in the protein degradation system of plants. To determine whether the nitrate-induced 1a-HIS protein degradation is depending on the proteasome pathway, a proteasome inhibitor MG132 was applied in the assay, while DMSO served as control. Total proteins extracted from KNO_3-treated 'GL3' leaves were pretreated with MG132 or DMSO for 30 min, and 1a-HIS fusion protein was added to those samples and detected as aforementioned. The results showed that addition of MG132 inhibited the 1a-HIS protein degradation largely, while DMSO had no effect on that (Fig. 2C). These data indicated that KNO_3-induced 1a-HIS protein degradation was most likely mediated by the proteasome pathway.

In addition, we also performed the cell-free degradation assay by using protein extracts from KNO_3- or KCl-treated apple calli to further confirm the nitrate-induced 1a-HIS protein degradation (Supplementary Fig. S2B and S2C). And similar results were obtained compared to that from the 'GL3' leaves. Collectively, these data indicated that nitrate treatment destablized viral protein 1a through UPS pathways.

ApNMV 1a interacts with MdBT2

To determine the protein(s) that mediates the degradation of ApNMV 1a under nitrate treatment, we performed an Y2H assay using 1a protein as bait to screen the apple cDNA library, and MdBT2 (MDP0000643281), a known nitrate-responsive protein, was identified as a potential prey. This protein contains an N-terminal BTB domain, a BACK-like domain in the middle, and a C-terminal TAZ domain (Fig. 3A). To confirm the protein interaction between ApNMV 1a and MdBT2, an Y2H assay was conducted. The coding sequences of 1a and MdBT2 were inserted into pGBT9 and pGAD424, respectively, and they were co-transformed into yeast cells. The result showed that the colonies grew normally in SD/-Trp/-Leu/-His/-Ade defective medium, suggesting the interaction between 1a and MdBT2 (Supplementary Fig. S3). In addition, we also tested interactions between MdBT2 and other vial components ($2a^{pol}$, MP, and CP) using Y2H assay, and found that MdBT2 only interacted with 1a but not with other viral proteins (Supplementary Fig. S3).

To identify the domain(s) that is required for interactions of the two proteins, we first chopped the MdBT2 into several fragments depending on the distribution of domains (Fig. 3A), and constructed them into pGBD vectors, while full-length of MdBT2 served as positive control. We found that the yeast grew on SD/-Trp/-Leu/-His/-Ade defective medium only when both BACK-like and TAZ domains were present, indicating these two domains were responsible for interacting with 1a (Fig. 3A). Similarly, we next splitted 1a into N-terminal MET domain and C-terminal HEL domain and found that neither of them interacted with MdBT2 (Fig. 3B), indicating the full-length of 1a was required for 1a-MdBT2 interactions.

We next utilized a BiFC assay to verify the 1a-MdBT2 interactions. The Agrobacterium harboring the MdBT2-nYFP and 1a-cYFP constructs were co-infiltrated into *N. benthamiana* leaves, and strong yellow fluorescence signals were captured in the cytoplasm under a confocal microscope (Fig. 3C, upper panel). However, when combined MdBT2-nYFP with cYPF (Fig. 3C, middle panel), or 1a-cYFP with nYFP (Fig. 3C, bottom panel), no signal was observed in neither of them. These data indicted that ApNMV 1a physically interacted with MdBT2 in the cytoplasm in vivo.

To further confirm the interactions between 1a and MdBT2, a pull-down assay was conducted. The fusion protein GST-1a or a simple GST was incubated with MdBT2-HIS and GSH-attached beads. Then target proteins were eluted with GSH solution and tested with anti-GST and anti-HIS antibodies. The results showed that the MdBT2-HIS fusion protein was pulled down in the presence of GST-1a but not GST (Fig. 3D), suggesting GST-1a interacted with MdBT2-HIS in vitro.

We finally determined the 1a-MdBT2 interactions using a luciferase complementation imaging assay. The Agrobacterium harboring MdBT2-nLuci and cLuci-1a were co-infiltrated into *N. benthamiana* leaves, and empty vectors served as control. The results showed that luminescent signals were observed only when both

MdBT2-nLuci and cLuci-1a were present, and no signal was captured in neither MdBT2-nLuci plus cLuci combination nor nLuci plus cLuci-1a combination (Fig. 3E), suggesting the interactions of 1a and MdBT2 in vivo. Collectively, all these data indicated that ApNMV 1a interacted with MdBT2 both in vivo and in vitro.

MdBT2 promotes ubiquitination and degradation of ApNMV 1a

Given that MdBT2 is one of the components of BTB/POZ type E3 ligase and functional in interacting with target proteins. We thus hypothesized that MdBT2 might promote the ubiqitination and degradation of its interacting partner ApNMV 1a. To verify our hypothesis, we first performed a cell-free degradation assay using the apple calli of wt,*MdBT2-OE* , and *MdBT2-anti* . The gene expression of*MdBT2* was increased in the overexpression calli but inhibited in the antisense compared to that of WT (Supplementary Fig. S4A), suggesting these calli were suitable for MdBT2 functional analysis. Then total protein extracts from these three types of apple calli were incubated with 1a-HIS fusion protein for different time points, respectively. After immunoblotted with anti-HIS antibody, we found that the degradation speed of 1a-HIS protein was faster in proteins extracted from *MdBT2-OE* transgenic calli (Fig. 4A, the middle section), but slower in protein extracts of *MdBT2-anti* (Fig. 4A, the right section) compared to that of WT (Fig. 4A, the left section). These data indicated that MdBT2 promoted 1a protein degradation in vitro. To testify whether proteasome is involved in 1a-HIS degradation, proteasome inhibitor MG132 was applied to these experiments, and the 1a-HIS protein degradation was inhibited in proteins from all the three types of apple calli (Fig. 4B), suggesting 26S proteasome pathway might be involved in MdBT2-mediated 1a-HIS protein degradation.

To further verify the role of MdBT2 in promoting ApNMV 1a protein degradation, we transformed Agrobacterium harboring pCXSN-1a-HA construct into 'GL3' apple plantlet leaves of WT, *MdBT2-OE* , and*MdBT2-anti* transiently via vaccum method. The transgenic apple plantlets were obtained previously from our lab, and we confirmed that*MdBT2-OE* transgenic plantlet had higher *MdBT2* gene expression level, while that was lower in the *MdBT2-anti*plantlets compared to that of WT (Supplementary Fig. S4B), suggesting these transgenic lines were suitable for MdBT2 functional analysis. Total proteins were extracted five days post-transformation and anti-HA antibody was used for immunoblotting. The results showed that 1a-HA protein level in *MdBT2-OE* leaves was lower than that of WT, but was higher in *MdBT2-anti* transgenic leaves compared with that of WT (Fig. 4C). Because the transcript level of 1a-HA was similar among the three types of leaves (Fig. 4D), we thus assumed that MdBT2 regulated the protein stability of 1a-HA in vivo.

We next tested whether ubiquitination was involved in MdBT2-mediated ApNMV 1a protein destablization. The active MdBT2-GFP proteins were first obtained via immunoprecipitating from total protein extracts of*MdBT2-OE* calli using anti-GFP antibody. Then 1a-HIS protein was incubated with human E1, E2, ubi, and active MdBT2-GFP in incubation buffer, and detected by anti-HIS and anti-Ubi antibodies. GFP proteins immunoprecipitated from 35S:GFP transgenic apple calli served as control. The results showed that high-molecular mass forms of 1a-HIS, which are polyubiquitinated 1a-HIS (Ubi(n)-1a-HIS), were detected in the presence of active MdBT2 proteins when immunoblotted by anti-HIS antibody (Fig. 4E, upper image). And a higher amount of ubiquitinated proteins were also detected in the presence of active MdBT2-GFP when immunoblotted using anti-Ubi antibody (Fig. 4E, lower image). These data suggested that MdBT2 was involved in promoting the ubiquitination of 1a-HIS in vitro.

To determine whether MdBT2 promotes the 1a-HIS protein ubiquitination in vivo, we transformed the pCXSN-1a-HA into apple plantlet leaves of 'GL3' WT, *MdBT2* -OE, and *MdBT2-anti* as aforementioned. After treatment with MG132, total protein extracts of the three types of apple leaves were immunoprecipitated with anti-HA antibody, then the precipitates were detected using anti-HA (Fig. 4F, upper image) and anti-Ubi (Fig. 4F, lower iamge) antibodies. We found that the amount of Ubi(n)-1a-HA were higher in *MdBT2-OE* leaves, but lower in*MdBT2* -anti leaves compared to that of WT (Fig. 4F), indicating that MdBT2 promoted the ubiquitination of 1a protein in vivo. Therefore, these data indicated that MdBT2 was involved in promoting 1a protein ubiquitination and degradation via UPS pathways.

MdCUL3A is not involved in MdBT2 mediated degradation of ApNMV 1a

In CRL3 type of E3 ligase complexes, BTB/POZ proteins usually serve as scaffold to link the target protein and CUL3 through physical protein interactions (Gingerich et al*.,* 2005; Hua and Vierstra, 2011). Previous reports have proved the interaction between MdBT2 and MdCUL3A through multiple methods (Zhao et al*.,* 2016; Wang et al.,2018), and we reconfirmed the interaction via a pull-down assay. Similar result was obtained that MdCUL3A-HIS protein was pulled down only in the presence of GST-MdBT2, suggesting the physical interaction of the two proteins (Supplementary Fig. S5A).

We next tested if MdCUL3A was involved in MdBT2-mediated 1a protein degradation. A cell-free degradation assay was conducted using total proteins extracted from the *MdCUL3A* -OE transgenic apple calli. The transcript level of *MdCUL3A* was higher in *MdCUL3A* -OE compared to that of WT apple calli (Supplementary Fig. S5B), suggesting these transgenic materials were suitable for functional analysis of MdCUL3A. After immunoblotted with anti-HIS antibody, we found the 1a-HIS protein degradation speed was similar in the proteins extracted from*MdCUL3A* -OE calli with that of WT (Fig. 5A), suggesting MdCUL3A might not be closely involved in MdBT2-mediated 1a protein degradation.

To explore the possible reasons for this, a competitive pull-down assay was conducted to test the effect of MdCUL3A on the 1a-MdBT2 interactions. The results showed that addition of increased amount of MdCUL3A-HIS protein decreased the quantity of MdBT2-HIS that was pulled down (Fig. 5B), suggesting the repression effects of MdCUL3A-HIS on the interactions between GST-1a and MdBT2-HIS, which might be a possible reason that MdCUL3A had no effect in MdBT2-mediated 1a degradation.

MdBT2 suppresses ApNMV genomic RNA accumulation by promoting 1a ubiquitination and degradation

Given that 1a plays critical roles in viral genomic RNA replication according to its closely related model virus BMV, we thus hypothesized that MdBT2-mediated 1a degradation might inhibit ApNMV genomic RNA replication in apple. To verify our hypothesis, we transformed the infectious clone of ApNMV into apple 'GL3' leaves of WT,*MdBT2-OE* , and *MdBT2-anti* via vacuum method. Five days post-transformation, the leaves were collected and prepared for extraction of total proteins and RNAs. We first tested the protein level of 1a using anti-1a specific antibody, and found that it was lower in*MdBT2-OE* leaves, but was higher in *MdBT2-anti* leaves compared to that of WT (Fig. 6A), suggesting MdBT2 promoted the protein degradation of 1a during virus infection. We next verify the ubiquitination of 1a mediated by MdBT2, and found that the amount of poly-ubiquitinated 1a was higher in *MdBT2-OE* , but lower in*MdBT2-anti* leaves compared to that of WT when detected with anti-1a antibody (Fig. 6B, upper image). Also, more ubiquitinated proteins were present in *MdBT2-OE* leaves, but less in*MdBT2-anti* leaves compared to that in WT when detected with anti-Ubi antibody (Fig. 6B, lower image), suggesting MdBT2 promoted ApNMV 1a protein ubiquitination and degradation during virus infection.

We then determined the role of MdBT2 in ApNMV viral RNA replication via Northern blot by using a DIG-labeled probe that targeting the CP-coding seqence of ApNMV. The results showed that accumulated viral RNA levels in *MdBT2-OE* leaves were lower, but they were higher in*MdBT2-anti* leaves compared to that in WT leaves (Fig. 6C), suggesting MdBT2 played a negative role in ApNMV replication in apple. These data indicated that MdBT2 might repress the ApNMV genomic RNA replication by promoting the ubiquitination and degradation of 1a protein.

MdBT2 interferes with the interactions between 1a and 2a^{pol}

We have previously identified the protein interactions between ApNMV 1a and 2a^{pol}, the homologous of both are required and sufficient to support viral genomic RNA replication in BMV case (Diaz and Wang, 2014; Zhang et al*.,* 2020). Given that 1a also interacted with MdBT2 (Fig. 3), we next asked whether MdBT2 affected the interaction between 1a and 2a^{pol}. We first performed a luciferase complementation imaging assay to explore the relationship of the three proteins. The interaction between 1a and 2a^{pol} was reconfirmed in the assay, and strong luminescent signals were observed only in the presence of both 1a-nLuci and cLuci-2a^{pol} (Fig. 7A). Then pCXSN-MdBT2-HA was introduced and co-infiltrated with 1a-nLuci and cLuci-2a^{pol} and observed under an in vivo imaging system. The results indicated that luminescent signals

were decreased progressively with the increased ratio of pCXSN-MdBT2-HA (Fig. 7B), suggesting that MdBT2-HA competed with $2a^{pol}$ and interfered with its interactions with 1a in vivo.

To further verify the interference of MdBT2 on the 1a-$2a^{pol}$ interactions, we next conducted a competitive pull-down assay using fusion proteins of GST-$2a^{pol}$, MdBT2-HIS, and 1a-HIS obtained from prokaryotic expression system. GST-$2a^{pol}$ and 1a-HIS were mixed and incubated with MdBT2-HIS and went through GST-attached column. With the addition of increasing amount of MdBT2-HIS protein, the amount of 1a-HIS protein pulled down decreased progressively, indicating that MdBT2-HIS competed with GST-$2a^{pol}$ to interact with 1a-HIS in vitro (Fig. 7C). In addition, we also observed that MdBT2-HIS was not pulled down by GST-$2a^{pol}$ (Fig. 7C), indicating they did not interact with each other, which was similar to what we found in Y2H assay (Supplementary Fig. S3). Thus, in addition to promoting 1a ubiquitination and degradation, MdBT2 might also inhibit ApNMV viral genomic RNA replication through interfering with the interactions between viral replication components 1a and $2a^{pol}$.

Discussion

As obligate parasites with limited genome, plant viruses interact extensively with their hosts to hijack the plant intracellular machinery for self survival and infection, which usually leads to disordered physiological responses and develops to visible diseases that compromising plants growth and development. For counteraction, plants employ multiple strategies to restrict viral infection, including gene silencing, hormone-mediated defense, immune receptor signaling, protein modification and degradation (Alcaide-Loridan and Jupin, 2012; Incarbone and Dunoyer, 2013; Korner et al*.,* 2013; Mandadi and Scholthof, 2013; Calil and Fontes, 2017). The UPS is a highly conserved protein degradation pathway among eukaryotes and is involved in regulating many cellular biological mechanisms, including defense responses against viruses (Alcaide-Loridan and Jupin, 2012; Zhou and Zeng, 2017).

To date, the UPS pathway has been reported to be involved in disrupting different stages in viral infection, such as viral genome replication and movement. For instance, UPS restricted the replication of turnip yellow mosaic virus (TYMV) by degrading and eliminating its RdRp accumulation during viral infection in Arabidopsis (Prod'homme et al*.,* 2001; Camborde et al*.,* 2010). A recent finding proved that an E3 ligase NbUbE3R1 (ubiquitin E3 ligase containing RING domain 1) functioned in inhibiting the replication of bamboo mosaic virus (BaMV), probably because of its interaction with the viral replicase (Chen et al*.,* 2019). And here we found that MdBT2 interacted with and promoted the ubiquitination and degradation of viral protein 1a, which plays an essential role in viral replication according to its homologous in BMV case (Diaz and Wang, 2014), to inhibit the replication of ApNMV in apple (Figs. 3, 4, and 6).

Upon establishment of infection in an individual cell, plant viruses spread from cell to cell to achieve a systemic infection, and MP plays a critical role in virus movement. Specifically, MP forms complexes with viral genome, and then increases the permeability of plasmodesmatal to allow the transportation of the complexes into neighboring cells (Lucas, 2006; Ueki and Citovsky, 2011). Thus, MPs are also potential substrates of UPS pathways in plant defense responses to control viral infection. For example, the MP of tobacco mosaic virus (TMV) (Reichel and Beachy, 2000), TYMV (Drugeon and Jupin, 2002), and potato leafroll virus (PLRV) (Vogel et al*.,* 2007) have been reported to be degraded by the UPS pathways. We also tested the protein interactions between ApNMV MP and MdBT2 to see if the latter is involved in regulating virus movement, but MdBT2 only interacted with 1a, but not with any other viral proteins, including the MP (Supplementary Fig. S3). Nevertheless, UPS pathway has been developed as one of the common strategies that plants utilized to defense virus infection.

BT2 was first identified in an Y2H assay to screen calmodulin-binding proteins (Du and Poovaiah, 2004), and it was later found to be involved in assembling of E3 ligase with CUL3 and RBX1, and functional in substrate recognition in model plant Arabidopsis (Figueroa et al*.,* 2005). Then, BT2 was proved to behave downstream of TAC1 to regulate induction of telomerase (Ren et al*.,* 2007), and also functioned in mediating responses to nutrients (nitrogen and sugar), hormones (auxin and ABA), and stresses (cold and H_2O_2) (Mandadi et al*.,* 2009). These evidences suggest that BT2 is a multifunctional protein in plant growth and development.

As a nitrate-responsive protein, BT2 coding gene expression is induced by nitrate in both Arabidopsis (Mandadi et al., 2009) and apple (Supplementary Fig. S1A). And recent findings suggest that MdBT2 regulates accumulation of anthocyanin and malate in apple through interacting with and degrading MdMYB1 (Wang et al., 2018), MdCIbHLH1 (Zhang et al., 2020 a), and MdMYB73 (Zhang et al., 2020 b), respectively, in response to nitrate. And here, we found that nitrate treatment promoted the protein degradation of viral protein 1a in vitro through proteasome pathway (Fig. 2; Supplementary Fig. S2), and overexpressing MdBT2 inhibited the viral RNA replication by targeting and degrading viral protein 1a (Figs. 4 and 6). These findings imply that moderately increased nitrate application might help to control ApNMV infection in apple cultivation. In addition to nitrate, and our recent findings demonstrate that MdBT2 plays critical roles in regulating cellular metabolisms in response to multiple environmental factors as a subunit of E3 ligase. For example, MdBT2 integrates the signals from ABA, wounding, drought, light, and UV-B to regulate biosynthesis and accumulation of anthocyanin by targeting and degrading bZIP44 (basic leucine zipper 44) (An et al., 2018), WRKY40 (An et al., 2019 b), ERF38 (ethylene response factor 38) (An et al., 2020 c), TCP46 (teosinte branched/cycloidea/proliferating 46) (An et al., 2020 d), and BBX22 (B-box 22) (An et al., 2019 c), respectively. In addition, MdBT2 was reported to regulate leaf senescence through MdbHLH93 (An et al., 2019 a), MdMYC2, and MdJAZ2 (JAZMONATE ZIM domain 2) (An et al., 2021). Collectively, these proofs suggested that MdBT2 serves as a signal hub to regulate cellular metabolisms in response to biotic and abiotic stresses.

MdBT2, a member of the BTB-TAZ subfamily, contains a N-terminal BTB domain, a BACK-like domain in the middle, and a C-terminal TAZ domain. As an adaptor protein in the CRL3 ligase complex, BT2 interacts with both CUL3 and potential substrate to mediated the target protein ubiquitination and degradation (Petroski and Deshaies, 2005). We found both the BACK-like and TAZ domains were responsible for interacting with ApNMV 1a (Fig. 3A). MdBT2 also interacted with MdCUL3A (Supplementary Fig. S5A), which has already been proved previously (Zhao et al., 2016; Wang et al., 2018). However, as a possible component of the E3 ligase, MdCUL3A had rare effect in 1a protein degradation in vitro (Fig. 5A), and MdCUL3A even competed with ApNMV 1a to interact with MdBT2 (Fig. 5B), indicating MdBT2 promotes 1a ubiquitination and degradation in an MdCUL3A-independent pathway. Actually, this has been reported in apple that MdBT2 promotes MdMYB1 degradation in an MdCUL3A-independent pathway (Wang et al., 2018). These findings suggest that MdBT2 might recruit some other, yet unknown, E3 ligases to mediate the ubiquitination and degradation of targets like MdMYB1 and viral 1a protein.

In the well-established model virus BMV, both 1a and $2a^{pol}$ are required and sufficient to support viral genome replication, and 1a-$2a^{pol}$ interactions play a critical role in this process (Diaz and Wang, 2014). Deletion of N-terminal of $2a^{pol}$, which is responsible for interacting with 1a, severely inhibits BMV viral RNA replication (Traynor et al., 1991; Kao and Ahlquist, 1992). Our previous findings revealed that the C-terminal of 1a and N-terminal of $2a^{pol}$ are required for 1a-$2a^{pol}$interaction (Zhang et al., 2020). We reported here that full-length 1a was required for interacting with MdBT2 (Fig. 3B), and increased amount of MdBT2 interfered with the interaction between 1a and $2a^{pol}$ (Fig. 7), which might be another possible reason that ApNMV viral replication was inhibited in *MdBT2-OE* transgenic apple leaves (Fig. 6C). In addition, 1a's inter- and intra-molecular interactions also play an important role in BMV replication (Diaz et al., 2012), and those interactions of ApNMV have been verified in our previous reports (Zhang et al., 2020), thus we predicted that the MdBT2-1a interaction may also interrupt the 1a's inter- or intra-molecular interactions, and lead to restricted viral RNA replication.

Nitrogen is a macronutrient for plant growth and development, and it is also involved in regulating interactions between the host plants and pathogens (Dordas, 2008). With the nature of available nitrogen in soil, lack or excess of nitrogen might modulate plant resistance through some yet unknown mechanisms to counteract pathogens (Huber and Wstson, 1974). Currently, NO, generated partially in nitrate assimilation by nitrate reductase, is a well-accepted compound that plays critical roles in plant immunity (Wendehenne et al., 2014). NO was first found to mediate defense reactions against bacterial in plants (Delledonne et al., 1998), and it was later demonstrated to active hypersensitive reaction to counteract pathogens in tobacco (Kumar and Klessig, 2000; Asai and Yoshioka, 2009), and enhanced NO content was proved to increase the

resistance to TMV (Klessig et al., 2000). What's more, NO also played a role in BR-mediated resistance against CMV and TMV in plants (Deng et al., 2016; Zou et al., 2018). Moreover, feeding the tobacco plants with nitrate could enhance the resistance to *Pseudomonas syringae* pv.*Phaseolicola* by increasing the accumulation of NO and SA, SA-mediated PR gene expression, as well as polyamine-mediated hypersensitive reactions (Gupta et al., 2013). And here, we found that increased nitrate favored the apple plantlets inhibit ApNMV genomic RNA replication through MdBT2-mediated ubiquitination and degradation of viral replication protein 1a. Of course, enhanced nitrate might also inhibit ApNMV genomic RNA replication through SA or NO signaling pathways, which is an interesting point and need further investigation to elucidate.

In sum, we identified a nitrate-responsive BTB domain-containing protein MdBT2 in apple, which inhibits the ApNMV viral RNA replication by mediating degradation of ApNMV 1a protein, as well as interfering with the interaction between viral replication proteins 1a and $2a^{pol}$. Our work provides the theoretical foundation to control apple mosaic disease in apple cultivation, and also determines a potential target gene that may be applied in genetic breeding to control apple mosaic disease in apple.

Supplementary Fig. S1 The gene expression of *MdBT2* (A) and *MdNRT1.1* (B) in response to KNO_3 and KCl. The apple plantlets were treated with KNO_3 or KCl with the indicated time, and samples were collected for RNA extraction. Then qRT-PCR were utilized to test the expression of the two genes. **, $P<0.01$; ***, $P<0.001$.

Supplementary Fig. S2 Protein degradation of 1a-HIS and $2a^{pol}$-HIS in vitro. A. $2a^{pol}$-HIS protein degradation in proteins extracted from 'GL3' leaves treated with KNO_3 or KCl. 1a-HIS protein degradation in proteins extracted from wt apple calli pretreated with KNO_3 or KCl in the absence (A) or presence (B) of MG132. The charts on the right side indicated the degradation trends in (A)-(C), and the intensity of protein bands at 0 h was set as 1.00. MdACTIN served as loading control.

Supplementary Fig. S3 A Y2H assay was used to test the interactions of MdBT2 with the four viral proteins, 1a, $2a^{pol}$, MP, and CP.

Supplementary Fig. S4 Using qRT-PCR to test the gene expression of *MdBT2* in transgenic apple calli (A) and GL3 shoots (B). *, $P<0.05$; ***, $P<0.001$.

Supplementary Fig. S5 MdBT2 interacts with MdCUL3A in vitro. A. Pull-down assay showed the in vitro interactions between GST-MdBT2 and MdCUL3A-HIS. The anti-GST and anti-HIS antibodies were used to detect the target proteins. GST-MdBT2, GST, MdCUL3A-HIS bands are indicated by short lines on the right side. B. Using qRT-PCR to test the expression of *MdCUL3A* in its overexression transgenic apple calli. ***, $P<0.001$.

Author contributions

ZZ, XFW, and YJH initiated and designed the research. ZZ, FJZ, PS, PFZ, and YHX performed the experiments. ZZ and YJH analyzed the data. ZZ and YJH wrote and revised the manuscript. CXY and YJH supervised the project.

References

Adams E H G, Spoel S H. (2018). The ubiquitin–proteasome system as a transcriptional regulator of plant immunity. Journal of Experimental Botany, 69, 4529-4537.

Alcaide-Loridan C, Jupin I. (2012). Ubiquitin and plant viruses, let's play together! Plant Physiology, 160, 72-82.

An J-P, Liu Y, Zhang X, Bi S, Wang X-F, You C-X, Hao Y. (2020 d). Dynamic regulation of anthocyanin biosynthesis at different light intensities by the BT2-TCP46-MYB1 module in apple. Journal of Experimental Botany, 71, 3094-3109.

An J-P, Wang X-F, Hao Y. (2020 a). BTB/TAZ protein MdBT2 integrates multiple hormonal and environmental signals to regulate anthocyanin biosynthesis in apple. Journal of Integrative Plant Biology, 62(11),

1643-1646.

An J-P, Wang X-F, Zhang X, Bi S, You C-X, Hao Y. (2019 c). MdBBX22 regulates UV-B-induced anthocyanin biosynthesis through regulating the function of MdHY5 and is targeted by MdBT2 for 26 proteasome-mediated degradation. Plant Biotechnology Journal, 17, 2231-2233.

An J-P, Wang X-F, Zhang X, You C-X, Hao Y. (2021). Apple MdBT2 protein negatively regulates jasmonic acid-triggered leaf senescence by modulating the stability of MYC2 and JAZ2. Plant, Cell & Environment, 44(1), 216-233.

An J-P, Yao J-F, Xu R-R, You C-X, Wang X-F, Hao Y-J. (2018). Apple bZIP transcription factor MdbZIP44 regulates abscisic acid-promoted anthocyanin accumulation. Plant, Cell and Environment, 41, 2678-2692.

An J-P, Zhang X, Bi S, You C-X, Wang X-F, Hao Y. (2019 a). MdbHLH93, an apple activator regulating leaf senescence, is regulated by ABA and MdBT2 in antagonistic ways. New Phytologist, 222, 735-751.

An J-P, Zhang X, Bi S, You C-X, Wang X-F, Hao Y. (2020 c). The ERF transcription factor MdERF38 promotes drought stress-induced anthocyanin biosynthesis in apple. Plant Journal, 101, 573-589.

An J-P, Zhang X, You C-X, Bi S, Wang X-F, Hao Y. (2019 b). MdWRKY40 promotes wounding-induced anthocyanin biosynthesis in association with MdMYB1 and undergoes MdBT2-mediated degradation. New Phytologist, 224, 380-395.

Asai S, Yoshioka H. (2009). Nitric oxide as a partner of reactive oxygen species participates in disease resistance to necrotrophic pathogen Botrytis cinerea in Nicotiana benthamiana. Molecular Plant Microbe Interaction, 22, 619-629.

Bachmair A, Novatchkova M, Potuschak T, Eisenhaber F. (2001). Ubiquitylation in plants: a post-genomic look at a post-translational modification. Trends in Plant Science, 6, 463-470.

Bujarski J, Figlerowicz M, Gallitelli D, Roossinck M, Scott S. (2012). Family Bromoviridae. Virus Taxonomy, Ninth Report of the International Committe on Taxonomy of Viruses. A. King, M. Adams, E. Carstens and E. Lefkowitz. London, Academic Press: 965-976.

Calil I, Fontes E. (2017). Plant immunity against viruses: antiviral immune receptors in focus. Annuals of Botany, 119, 711-723.

Camborde L, Planchais S, Tournier V, Jakubiec A, Drugeon G, Lacassagne E, Pflieger S, Chenon M, Jupin I. (2010). The ubiquitin-proteasome system regulates the accumulation of turnip yellow mosaic virus RNA-dependent RNA polymerase during viral infection. The Plant Cell, 22, 3142-3152.

Chen H, Zou Y, Shang Y, Lin H, Wang Y, Cai R, Tang X, Zhou J. (2008). Firefly luciferase complementation imaging system assay for protein-protein interactions in plants. Plant Physiology, 146, 368-376.

Chen I-H, Chang J-E, Wu C-Y, Huang Y-P, Hsu Y-H, Tsai C-H. (2019). An E3 ubiquitin ligase from Nicotiana benthamiana targets the replicase of bamboo mosaic virus and resticts its replication. Molecular Plant Pathology, 20, 673-684.

Chen S, Songkumarn P, Liu J, Wang G. (2009). A versatile zero background T-vector system for gene cloning and functional genomics. Plant Physiology 150, 1111-1121.

Dai H, Li W, Han G, Yang Y, Ma Y, Li H, Zhang Z. (2013). Development of a seedling clone with high regeneration capacity and susceptibility to Agrobacterium in apple. Scientia Horticulturae, 164, 202-208.

Delledonne M, Xia Y, Dixon RA, Lamb C. (1998). Nitric oxide functions as a signal in plant disease resistance. Nature, 394, 585-588.

Deng X, Zhu T, Zou L, Han X, Zhou X, Xi D, Zhang D, Lin H. (2016). Orchestration of hydrogen peroxide and nitric oxide in brassinosteroid-mediated systemic virus resistance in Nicotiana benthamiana. Plant Journal, 85, 478-493.

Diaz A, Gallei A, Ahlquist P. (2012). Bromovirus RNA replication compartment formation requires concerted action of 1a's self-interacting RNA capping and helicase domains. Journal of Virology, 86, 821-834.

Diaz A, Wang X. (2014). Bromovirus-induced remodeling of host membranes during viral RNA replication. Current Opinion in Virology, 9, 104-110.

Dordas C. (2008). Role of nutrients in controlling plant diseases in sustainable agriculture, A review. Agron. Sustain. Dev, 28, 33-46.

Drugeon G, Jupin I. (2002). Stability in vitro of the 69K movement protein of turnip yellow mosaic virus is regulated by the ubiquitin-mediated proteasome pathway. Journal of general virology, 83, 3187-3197.

Du L, Poovaiah B. (2004). A novel family of Ca2+/calmodulin-binding proteins involved in transcription regulation: interaction with fsh/Ring3 class transcription activatiors. Plant Molecular Biology, 54, 549-569.

Figueroa P, Gusmaroli G, Serino G, Habashi J, Ma L, Shen Y, Feng S, Bostick M, Callis J, Hellmann H, Deng X W. (2005). Arabidopsis Has Two Redundant Cullin3 Proteins That Are Essential for Embryo Development and That Interact with RBX1 and BTB Proteins to Form Multisubunit E3 Ubiquitin Ligase Complexes in Vivo. The Plant Cell, 17, 1180-1195.

Genschik P, Sumara I, Lechner E. (2013). The emerging family of CULLIN3-RING ubiquitin ligases (CRL3s): cellular functions and disease implications. EMBO J, 32, 2307-2320.

Gingerich D J, Gagne J, Salter D, Hellmann H, Estelle M, Ma L, Vierstra R D. (2005). Cullins 3a and 3b assemble with members of the broad complex/tramtrack/bric-a-brac (BTB) protein family to form essential ubiquitin-protein ligases (E3s) in Arabidopsis. Journal of biological chemistry, 280, 18810-18821.

Gupta K, Brotman Y, Segu S, Zeier T, Zeier J, Persijn S, Cristescu SM, Harren FJM, Bauwe H, Fernie AR, Kaiser WM, Luis AJM. (2013). The form of nitrogen nutrition affects resistance against *Pseudomonas syringae* pv. *phaseolicola* in tobacco. Journal of Experimental Botany, 64(2), 553-568.

Han P, Wang C, Liu X, Dong Y, Jiang H, Hu D, Hao Y. (2019). BTB-BACK domain E3 ligase MdPOB1 suppresses plant pathogen defense against Botryosphaeria dothidea by ubiquitinating and degrading MdPUB29 protein in apple. Plant and Cell physiology, 60, 2129-2140.

Ho C, Lin S, Hu H, Tsay Y. (2009). CHL1 functions as a nitrate sensor in plants. Cell, 138, 1184-1194.

Hotton S, Callis J. (2008). Regulation of cullin RING ligases. Annual Review of Plant Biology, 59, 467-489.

Hua Z, Vierstra R D. (2011). The cullin-RING ubiquitin-protein ligases. Annual Review of Plant Biology, 62, 299-334.

Huber DM, and Watson RD. (1974). Nitrogen form and plant disease. Annu Rev Phytopathol, 12, 139-165.

Incarbone M, Dunoyer P. (2013). RNA silencing and its suppression: novel insights from in planta analysis. Trends in Plant Science, 18, 382-392.

Kao C C, Ahlquist P. (1992). Identification of the domains required for direct interaction of the helicase-like and polymerase-like RNA replication proteins of brome mosaic virus. Journal of Virology, 66, 7293-7302.

Klessig DF, Durner J, Noad R, Navarre DA, Wendehenne D, Kumar D, Zhou JM, Shah J, Zhang S, Kachroo P. (2000). Nitric oxide and salicylic acid signaling in plant defense. Proc Natl Acad Sci USA, 97, 8849-8855.

Kohrer K, Domdey H. (1991). Preparation of high molecular weight RNA. Methods Enzymol, 194, 398-405.

Korner C, Klause D, Niehl A, Dominguez-Ferreras A, Chinchilla D, Boller T, Heinlein M, Hann D. (2013). The immunity regulator BAK1 contributes to resistance against diverse RNA viruses. Molecular Plant Microbe Interaction, 26, 1271-1280.

Kumar D, Klessig DF. (2000). Differential induction of tobacco MAP kinases by the defense signals nitric oxide, salicylic acid, ethylene, and jasmonic acid. Molecular Plant Microbe Interaction, 13, 347-351.

Kunz S, Gardeström P, Pesquet E, Kleczkowski L A. (2015). Hexokinase 1 is required for glucose-induced repression of bZIP63, At5g22920, and BT2 in Arabidopsis. Frontiers in Plant Science, 6, 525.doi: 10.3389/fpls.2015.00525.

Lucas W. (2006). Plant viral movement proteins: agents for cell-to-cell trafficking of viral genomes. Virology, 344, 169-184.

Mandadi K K, Misra A, Ren S, McKnight T D. (2009). BT2, a BTB protein, mediates multiple responses to nutrients, stresses, and hormones in Arabidopsis. Plant Physiology, 150, 1930-1939.

Mandadi K K, Scholthof K-B. (2013). Plant immune responses against viruses: how does a virus cause disease? The Plant Cell 25, 1489-1505.

Mazzucotelli E, Belloni S, Marone D, De Leonardis A, Guerra D, Di Fonzo N, Cattivelli L, Mastrangelo A. (2006). The e3 ubiquitin ligase gene family in plants: regulation by dagradation. Current Genomics, 7, 509-522.

Metzger M, Pruneda J, Klevit R, Weissman A. (2014). RING-type E3 ligases: master manipulators of E2 ubiquitin-conjugating enzymes and ubiquitination. Biochim. Biophy. Acta, 1843, 47-60.

Misra A, McKnight T D, Mandadi K K. (2018). Bromodomain proteins GTE9 and GTE11 are essential for specific BT2-mediated sugar and ABA responses in Arabidopsis thaliana. Plant Molecular Biology, 96, 393-402.

Noda H, Yamagishi N, Yaegashi H, Xing F, Xie J, Li S, Zhou T, Ito T, Yoshikawa N. (2017). Apple necrotic mosaic virus, a novel ilarvirus from mosaic-diseased apple trees in Japan and China. Journal of General Plant Pathology, 83, 83-90.

Orosa B, He Q, Mesmar J, Gilroy E, McLellan H, Yang C, Craig A, Bailey M, Zhang C, Moore J, Boevink P, Tian Z, Birch P, Sadanandom A. (2017). BTB-BACK domain protein POB1 suppresses immue cell death by targeting ubiquitin E3 ligase PUB17 for degradation. PLoS Genetics, 13(1), e1006540. doi: 10.1371/journal.pgen.1006540.

Petroski M, Deshaies R. (2005). Function and regulation of cullin-RING ubiquitin ligases. Nature Review of Molecular Cell Biology, 6, 9-20.

Prod'homme D, Le Panse S, Drugeon G, Jupin I. (2001). Detection and subcellular localization of the turnip yellow mosaic virus 66K replication protein in infected cells. Virology, 281, 88-101.

Reichel C, Beachy R. (2000). Degradation of tobacco mosaic virus movement protein by the 26S proteasome. . Journal of Virology, 74, 3330-3337.

Ren S, Mandadi K K, Boedeker A L, Rathore K S, McKnight T D. (2007). Regulation of telomerase in Arabidopsis by BT2, an apparent target of TELOMERASE ACTIVATOR1. The Plant Cell, 19, 23-31.

Scheible W, Morcuende R, Czechowski T, Fritz C, Osuna D, Palacios-Rojas N, Schindelasch D, Thimm O, Udvardi M, Stitt M. (2004). Genome-wide reprogramming of primary and secondary metabolism, protein synthesis, cellular growth processes, and the regulatory infrastructure of Arabidopsis in response to nitrogen. Plant Physiology, 136, 2483-2499.

Traynor P, Young B, Ahlquist P. (1991). Deletion analysis of brome mosaic virus 2a protein: effects on RNA replication and systemic spread. Journal of Virology, 65, 2807-2815.

Ueki S, Citovsky V. (2011). To gate, or not to gate: regulatory mechanisms for intercellular protein transport and virus movement in plants. Molecular Plant, 4, 782-793.

Vierstra R D. (2009). The ubiquitin-26S proteasome system at the nexus of plant biology. Nature Reviews Molecular Cell BiolOgy, 10, 385-397.

Vogel F, Hofius D, Sonnewald U. (2007). Intracellular trafficking of potato leafroll virus movement protein in transgenic Arabidopsis. Traffic, 8, 1205-1214.

Walter M, Chaban C, Schutze K, Batistic O, Weckermann K, Nake C, Blazevic D, Grefen C, Schumacher K, Oecking C, Harter K, Kudla J. (2004). Visualization of protein interactions in living plant cells using bimolecular fluorescence complementation. Plant Journal, 40, 428-438.

Wang F, Zhu D, Huang X, Li S, Gong Y, Yao Q, Fu X, Fan L, Deng X. (2009). Biochemical insights on degradation of Arabidopsis DELLA proteins gained from a cell-free assay system. The Plant Cell, 21, 2378-2390.

Wang X-F, An J-P, Liu X, Su L, You C-X, Hao Y. (2018). The nitrate-responsive protein MdBT2 regulates anthocyanin biosynthesis by interacting with the MdMYB1 transcription factor. Plant Physiology, 178, 890-906.

Wendehenne D, Gao Q, Kachroo A, Kachroo P. (2014). Free redical-mediated systemic immunity in plants. Current Opinion in Plant Biology, 20C, 127-134.

Wendehenne D, Lamotte O, Frachisse JM, Barbier-Brygoo H, Pugin A. (2002). Nitrate efflux is an essential component of the cryptogein signaling pathway leading to defense responses and hypersensitive cell death in tobacco. The Plant Cell, 14, 1937-1951.

Xing F, Robe B L, Zhang Z, Wang H, Li S. (2018). Genomic Analysis, Sequence Diversity, and Occurrence of Apple necrotic mosaic virus, a Novel Ilarvirus Associated with Mosaic Disease of Apple Trees in China. Plant Disease, 102, 1841-1847.

Zhang Q, Gu K, Cheng L, Wang J, Yu J, Wang X-F, You C-X, Hu D, Hao Y. (2020 a). BTB-TAZ domain protein MdBT2 modulates malate accumulation and vacuolar acidification in response to nitrate. Plant Physiology, 183, 750-764.

Zhang Q, Gu K, Wang J, Yu J, Wang X-F, Zhang S, You C-X, Hu D, Hao Y. (2020 b). BTB-BACK-TAZ domain protein MdBT2-mediated MdMYB73 ubiquitination negatively regulates malate accumulation and vacuolar acidification in apple. Horticulture Research, 7, 151.

Zhang Z, Zhang F, Zheng P, Xie Y, You C-X, Hao Y. (2020). Determination of protein interactions among replication componets of apple necrotic mosaic virus. Viruses, 12, 474.

Zhao Q, Ren Y, Wang Q, You C-X, Hao Y. (2016). Ubiquitination-related MdBT scaffold protein target a bHLH transcription factor for iron homeostasis. Plant Physiology, 173, 1973-1988.

Zhou B, Zeng L. (2017). Conventional and unconventional ubiquitination in plant immunity. Molecular Plant Pathology, 18, 1313-1330.

Zou L, Deng X, Zhang L, Zhu T, Tan W, Muhammad A, Zhu L, Zhang C, Zhang D, Lin H. (2018). Nitric oxide as a signaling molecule in brassinosteroid-mediated virus resistance to cucumber mosaic virus in Arabidopsis thaliana. Physiologia Plantarum, 163, 196-210.

Figure legends

Fig. 1 Nitrate treatment inhibits ApNMV viral RNA accumulation in *Malus domestica*. A. Schematic model of infectious clone construction of ApNMV. The three RNA segments were constructed into binary vector, respectively.In the constructions, the three segments are driven by double CaMV 35S promoter, and are followed by a ribozyme (Rz) and a Nos terminator (Tnos). B. ApNMV RNA accumulation in leaves of 'GL3' treated with KNO_3. The infectious clone of ApNMV was used to agro-infiltrate the 'GL3' leaves under indicated concentration of KNO_3, and the leaves were collected for RNA extraction 4 days post-infiltration. DIG-labeled probes targeting the CP-coding sequence was used to test the RNA levels of (+)RNA3 and (+)RNA4 in a Northern blot assay with two duplicates for each treatment. The digits

(Mean±SD) indicate the signal intensity of (+)RNA3 and the band intensity of 0 mM were set as 100. The rRNA served as loading control. The experiment was repeated three times.

Fig. 2 Nitrate treatment destablizes viral protein 1a through the UPS pathways. A. Protein levels of 1a in leaves of 'GL3' treated with KNO_3. The infectious clone of ApNMV was used to agro-infiltrate the 'GL3' leaves under indicated concentration of KNO_3, and the leaves were collected for protein extraction 4 days post-infiltration. Anti-1a specific antibody was used in a Western blot assay with two duplicates for each treatment. MdACTIN served as loading control. The digits (Mean±SD) indicate the signal intensity and the band intensity of 0 mM were set as 1.00. B. 1a-HIS protein degradation in a cell-free degradation assay. 1a-HIS protein obtained from prokaryotic expression were embedded with total proteins extracted from apple callus treated with KCl or KNO_3 at the indicated time points. The protein samples were then subjected to a Western blot detection with anti-HIS antibody. MdACTIN served as loading control. C. 1a-HIS protein degradation in the proteins extracted from KNO_3-pretreated aplle callus in the absence or presence of MG132. The samples were collected at the indicated time points and subjected to a Western blot detection with anti-HIS antibody. MdACTIN served as loading control. The charts on the right side of indicated the degradation trends in (B) (upper chart) and (C) (bottom chart), respectively. The intensity of protein bands at 0 h was set as 1.00. All experiments were repeated three times independently.

Fig. 3 MdBT2 interacts with ApNMV 1a in vivo and in vitro. (A) and (B) illustrated the interactions between MdBT2 and 1a. MdBT2 (A) and 1a (B) was truncated into different fragments based on the domain structure, and different color on the left side indicates different domains that were included in the assay. Different combinations of constructs were transformed in yeast cells and cultured on selective medium SD-Trp/-Leu (SD-T-L), and interactions were tested on selective medium SD-Trp/-Leu/-His/-Ade (SD-T-L-H-A). The images were taken 3 d after incubation at 30 . C. BiFC assay indicated the interactions of MdBT2 and 1a in *N. benthamiana* cells. The nuclear was stained with DAPI (4',6-diamidino-2-phenylindole). BF, bright filed. Scale bar, 10 μm. D. Pull-down assay showed the in vitro interactions between MdBT2 and 1a. MdBT2-HIS protein was incubate with GST-1a or only GST proteins and went through the GST-attached column. Anti-GST and anti-HIS antibodies were used to detect the target proteins. GST-1a, GST, MdBT2-HIS bands are indicated by arrows on the left side. The ladder on the right side indicated the molecular weight (KDa) of target proteins. E. Luciferase complementation imaging assays indicated the interactions between MdBT2 and 1a in *N. benthamiana* cells. The bar on the right side indicates the intensity of the signals captured. Empty nLuci and cLuci vectors served as control. The images displayed here are representative of three independent experiments.

Fig. 4 MdBT2 promotes the ubiquitinatin and degradation of 1a in vivo and in vitro. 1a protein degradation in total proteins extracted from different transgenic apple calli in the absence (A) or presence (B) of MG132 in a cell-free protein degradation assay. 1a-HIS protein was incubated with protein extracts from transgenic (MdBT2-OE and MdBT2-anti) and WT apple calli with the indicated time. Anti-HIS was used to detect the target proteins. MdActin served as loading control. The charts on the right side showed the protein degrading trends in (A) (upper chart) and (B) (lower chart), and the intensity of protein bands of 0 h was set as 1.00. The 35S:1a-HA construct was transiently expressed in WT, MdBT-OE, and MdBT2-anti 'GL3' leaves, and the leaves were collected for protein (C) and RNA (D) extraction 5 d post agro-infiltration. Anti-HA antibody was used to detect the 1a-HA protein in a Western blot assay (C). MdACTIN served as loading control. qRT-PCR was used to detect the transcript level of 1a-HA (D). The 1a transcript level of the first duplicate in WT was set as 1.00. E. MdBT2 mediated the 1a protein ubiquitination in vitro. Active MdBT2-GFP protein was immunoprecipitated from *35S ::MdBT2-GFP* transgenic apple calli using anti-GFP antibody, and incubated with 1a-HIS protein, E1, E2, and ubiquitin in vitro. GFP protein immunoprecipitated from*35S ::GFP* transgenic apple calli served as control. Anti-HIS (upper panel) and anti-Ubi (lower panel) antibodies were used to detect the target proteins. Anti-GFP antibody was used to detect the input of GFP and active MdBT2-GFP proteins. The 1a-HIS and Ubi(n)-1a-HIS were labeled on the left side. F. MdBT2 mediated the 1a-HA protein ubiquitination in vivo. 35S::1a-HA construct was transiently expressed in WT, MdBT2-OE and MdBT2-anti 'GL3' leaves, and the samples were collected for protein extraction 4 d post-infiltration. Anti-HA antibody was used for immunoprecipitation (IP), anti-HA

(upper panel) and anti-Ubi (lower panel) antibodies were used for immunoblot (IB). Input indicated the samples collected before IP and detected with anti-ACTIN antibody. The 1a-HA and Ubi(n)-1a-HA were labeled on the left side. All the images showed here are representative of three independent experiments.

Fig. 5 MdBT2 promoted 1a degradation in an MdCUL3A-independent pathway. A. In vitro degradation of 1a-HIS in proteins extracted from MdCUL3A overexpression (MdCUL3A-OE) and WT apple calli. Prokaryotic expression system-obtained 1a-HIS protein was incubated with protein extracts from WT or MdCUL3A-OE for the indicated time in the presence of translation inhibitor cycloheximide (CHX). MdACTIN served as loading control. The chart on the right side indicates the protein degradation trend, and protein band intensity of 0 h was set as 1.00. B. Competitive pull-down assay showed the effect of MdCUL3A-HIS on the interactions between GST-1a and MdBT2-HIS. GST-1a and MdBT2-HIS proteins were incubated with different amount of MdCUL3A-HIS protein, and went through the GST-attached column. A simple HIS-tag protein served as control when MdCUL3A-HIS was absent. For the amount of MdCUL3A-HIS, single '+' means 2 μg protein, and '+ + +' indicates 6 μg protein. Anti-HIS antibody was used to detect both the MdCUL3A-HIS and MdBT2-HIS proteins. All the experiments were repeated three times and the images displayed were the representatives.

Fig. 6 MdBT2 inhibits ApNMV genomic RNA replication by promoting the degradation and ubiquitination of viral protein 1a. Infectious clone of ApNMV was agro-infiltrated into leaves of WT, MdBT2-OE, and MdBT2-anti, and total proteins (A and B) and RNAs (C) were extracted 5 d post-infiltration for further investigation. A. 1a protein levels in wt,*MdBT2-OE* , and *MdBT2-anti* transgenic plantlets leaves. Anti-1a specific antibody was used to detect 1a protein. MdACTIN served as loading control. The digits indicated the intensity of bands and the WT were set at 1.00. B. MdBT2 mediated the 1a protein ubiquitination in vivo. Total proteins were extracted and anti-1a antibody was used for immunoprecipitation (IP); anti-1a (top panel) and anti-Ubi (bottom panel) antibodies were used for immunoblot (IB) to test the target proteins. Input indicated the samples collected before IP and detected with anti-ACTIN antibody. The 1a and poly-ubiquitinated 1a (Ubi(n)-1a) were labeled on the left side. C. Detection of ApNMV genomic RNA accumulation in wt, *MdBT2-OE* , and *MdBT2-anti* transgenic plantlets leaves via Northern blot. Total RNAs were extracted using hot phenol method. DIG-labeled probes targeting the CP-coding sequence was used to test the (+)RNA3 and (+)RNA4 of ApNMV. The digits indicated the signal intensity of (+)RNA3, and the band intensity of WT were set as 100. The rRNA served as loading control. All the images displayed are representative of three independent experiments.

Fig. 7 MdBT2 interferes with the interactions between 1a and 2a^{pol}. A. 1a interacts with 2a^{pol}in *N. benthamiana* cells in a luciferase complementation imaging assay. Agrobacterium harboring different combinations were co-infiltrated into different parts of the same *N. benthamiana*leaf, and the iamges were taken 3 d post-infiltration under an in vivo imaging system after the leaves were incubated with the substrate of luciferase in dark for 3 min. B. A luciferase complementation imaging assay showed the affect of MdBT2-HA protein on the interactions between 1a and 2a^{pol}. Agrobacterium harboring 1a-nluci and cluci-2a^{pol} were mixed and co-infiltrated with agrobacteriun containing pCXSN-MdBT2-HA or pCXSN-HA. Increased ratio of pCXSN-MdBT2-HA was added into the mix from 1:1:1 (indicating the OD_{600} of the three are the same) to 1:1:5 (indicating the OD_{600} of pCXSN-MdBT2-HA was five time of 1a-nluci and cluci-2a^{pol}). Different combinations were illustrated on the right side of the image. The bars on the right side of (A) and (B) indicate the intensity of the signals captured. The empty nLuci and cLuci vectors served as control. C. Competitive pull-down assay showed the effect of MdBT2-HIS on the interactions between GST-2a^{pol} and 1a-HIS. Same amount of GST-2a^{pol} and 1a-HIS were mixed and incubated with different amount of MdBT2-HIS protein and went through GST-attached column. For the amount of MdBT2-HIS, '+' indicated 2 μg protein, and '+ + +' indicates 6 μg protein. A simple HIS-tag protein served as control when MdBT2-HIS was absent. Anti-HIS antibody was used to detect the 1a-HIS and MdBT2-HIS proteins. All the experiments were repeated three times and the images displayed were the representatives.

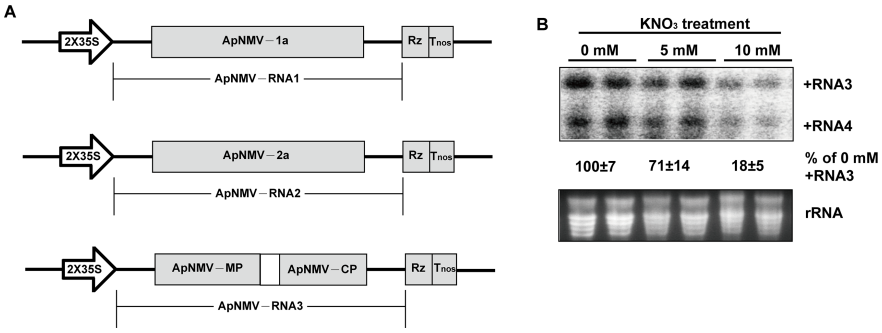

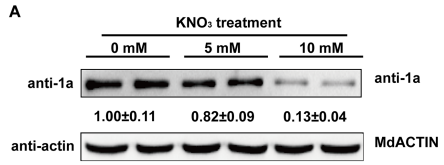

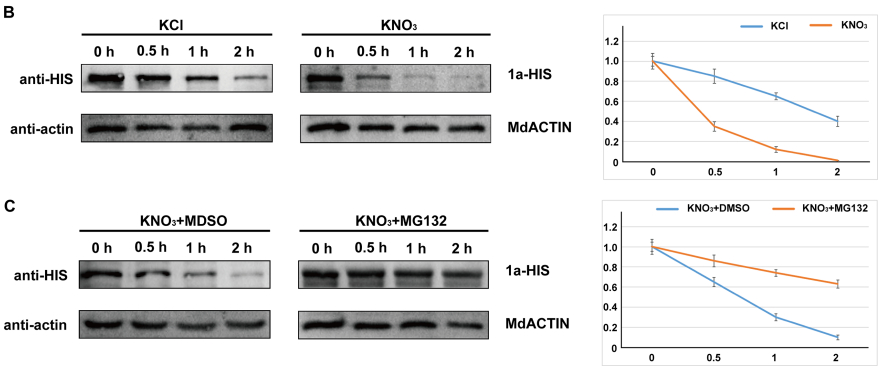

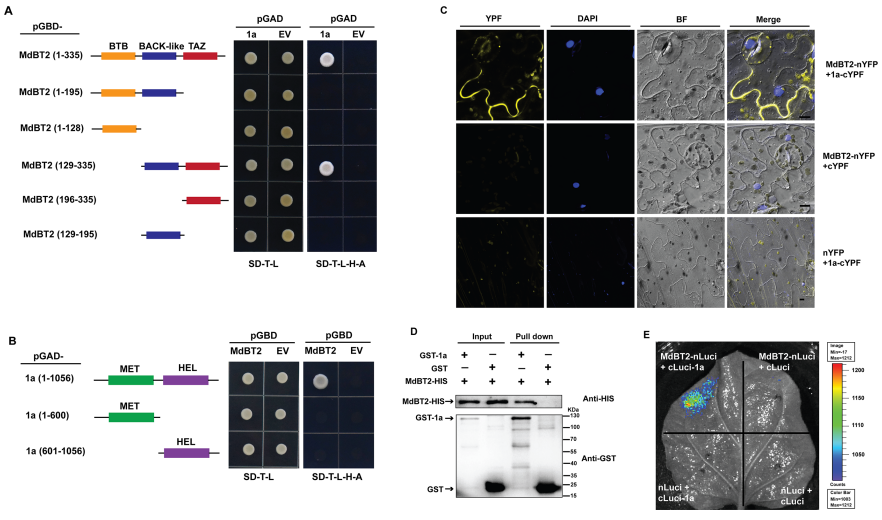

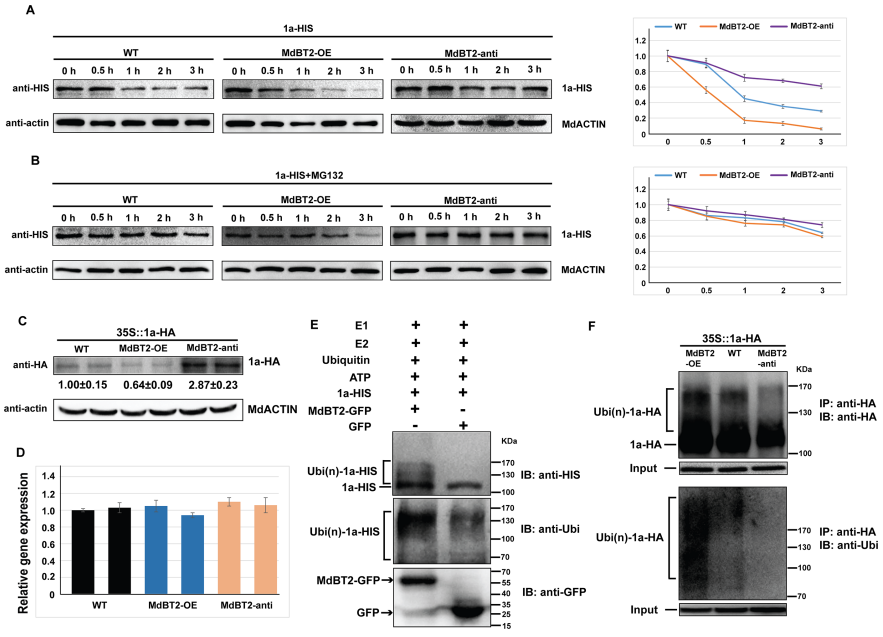

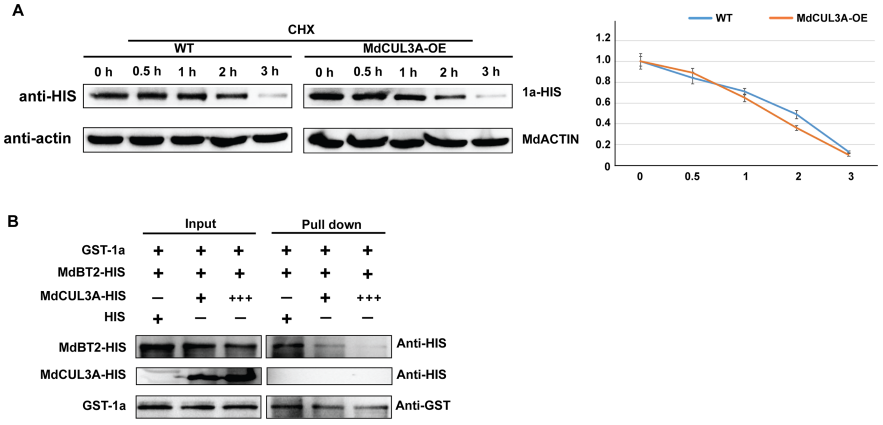

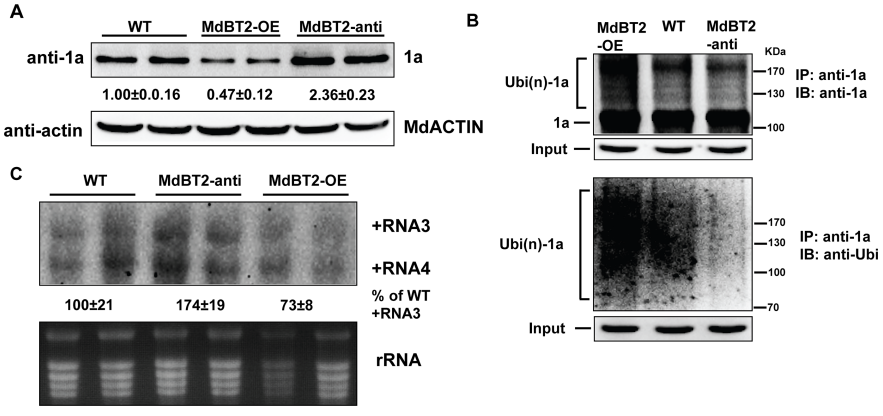

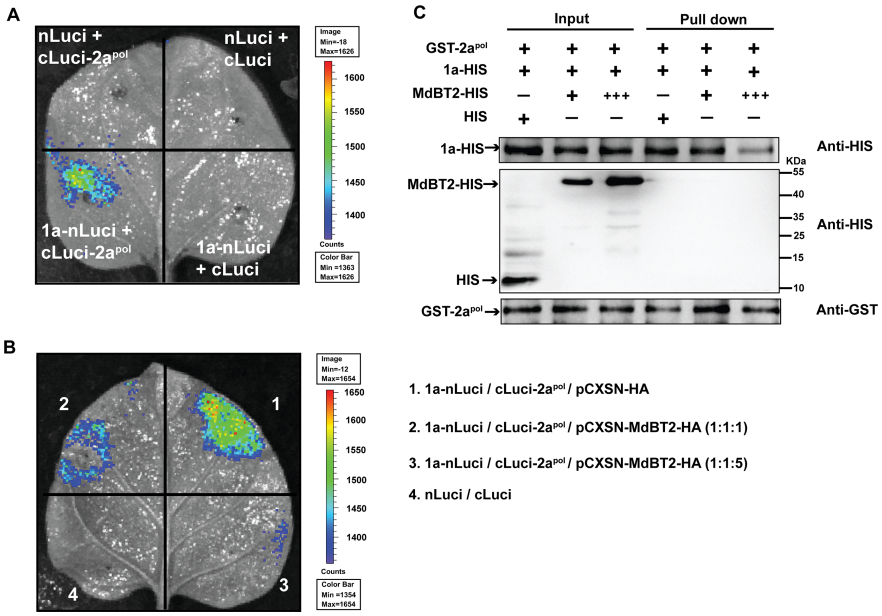

1. 1a-nLuci / cLuci-2a^{pol} / pCXSN-HA

2. 1a-nLuci / cLuci-2a^{pol} / pCXSN-MdBT2-HA (1:1:1)

3. 1a-nLuci / cLuci-2a^{pol} / pCXSN-MdBT2-HA (1:1:5)

4. nLuci / cLuci